Neuron, Vol. 15, 951–960, October, 1995, Copyright © 1995 by Cell Press

Modulation of K^+ Current by Frequency and External $[K^+]$: A Tale of Two Inactivation Mechanisms

Thomas Baukrowitz and Gary Yellen
Department of Neurobiology
Harvard Medical School
Massachusetts General Hospital
Boston, Massachusetts 02114

Summary

Voltage-activated K^+ currents and their inactivation properties are important for controlling frequency-dependent signaling in neurons and other excitable cells. Two distinct molecular mechanisms for K^+ channel inactivation have been described: N-type, which involves rapid occlusion of the open channel by an intracellular tethered blocker, and C-type, which involves a slower change at the extracellular mouth of the pore. We find that frequency-dependent cumulative inactivation of Shaker channels is very sensitive to changes of extracellular $[K^+]$ in the physiological range, with much more inactivation at low $[K^+]_{out}$, and that it results from the interaction of N- and C-type inactivation. N-type inactivation enhances C-type inactivation by two mechanisms. First, it inhibits outward K^+ flux, which normally fills an external ion site and thus prevents C-type inactivation. Second, it keeps the channel's activation gate open even after repolarization, allowing C-type inactivation to occur for a prolonged period.

Introduction

Voltage-activated K^+ channels are important not only for the repolarizing phase of the action potential, but also for determining the response of neurons to input stimuli and for the rhythmic signaling properties of neurons (Connor and Stevens, 1971; Aldrich et al., 1979; Hille, 1992). Outward K^+ currents generally oppose the action of excitatory stimuli, but this opposition disappears when prolonged depolarization or frequent activity produces K^+ channel inactivation. Inactivation during a single depolarizing stimulus action controls the utilization time for response to that stimulus (Connor and Stevens, 1971). During repetitive activity, K^+ channel inactivation progresses and accumulates; this cumulative inactivation can produce significant changes in signaling properties such as firing rate and action potential duration.

Inactivation of K^+ channels occurs by at least two distinct molecular mechanisms termed N- and C-type inactivation. N-type inactivation is usually quite rapid, with a time constant of several milliseconds, and occurs by a "ball-and-chain" mechanism: the N-terminal domain of the channel protein acts as a tethered blocker that occludes the pore after the activation gates open (Armstrong and Bezanilla, 1977; Hoshi et al., 1990; Zagotta et al., 1990; Demo and Yellen, 1991). C-type inactivation is generally slower to occur and slower to recover than N-type inactivation, and appears to involve structural changes at the extracellular mouth of the channel (Grissmer and Cahalan, 1989; Choi et al., 1991; Hoshi et al., 1991; Yellen et al., 1994). Most studies of C-type inactivation have been done in the absence of N-type inactivation, in channels that lack N-type inactivation either naturally or because of mutations that eliminate N-type inactivation. Studies on C-type inactivation in the Shaker K^+ channel with such an N-terminal deletion (Shaker H4:Δ6–46; here called ShΔ) show that this mechanism has little voltage dependence and a clear but relatively small sensitivity to external K^+ concentration ($[K^+]_{out}$; Hoshi et al., 1991; López-Barneo et al., 1993).

C-type inactivation can also be studied in the presence of N-type inactivation by focusing on the decay of the small remaining percentage of the current, after N-type inactivation has reached steady-state. Hoshi et al. (1991) noticed that C-type inactivation observed in this way was severalfold faster than C-type inactivation in isolation and concluded that the two mechanisms must be coupled in some way.

We have studied the cumulative inactivation of the Shaker K^+ channel that occurs with moderate repetitive stimulation (up to 2 Hz). Such cumulative inactivation requires slow recovery from inactivation, as seen with C-type inactivation, but with more rapid onset than usually seen for C-type inactivation. We find substantial cumulative inactivation that is accentuated at low $[K^+]_{out}$ and inhibited by increased $[K^+]_{out}$ in the physiological range of $[K^+]$. This K^+-inhibited cumulative inactivation depends on the presence of both inactivation mechanisms, as we demonstrate by mutations that remove each mechanism separately.

We find that K^+-inhibited cumulative inactivation is produced by two interactions between the N- and C-type inactivation mechanisms. First, N-type inactivation reveals the intrinsic $[K^+]_{out}$ sensitivity of C-type inactivation. Binding of K^+ or tetraethylammonium (TEA) to a site in the outer mouth inhibits C-type inactivation. This $[K^+]_{out}$ sensitivity is present when C-type inactivation is studied alone, but it is usually obscured by the outward flow of K^+. Even with little or no external K^+, the outward flow through an individual K^+ channel raises the local $[K^+]_{out}$ high enough to slow C-type inactivation substantially. The long-lasting block of an individual channel by the N-type inactivation particle eliminates this outward flux and allows C-type inactivation to be controlled exclusively by the global $[K^+]_{out}$, which is generally lower.

The second effect of N-type inactivation is to prolong the period during which C-type inactivation occurs. The binding of the N-type inactivation particle holds the activation gates open even after repolarization (Demo and Yellen, 1991; Ruppersberg et al., 1991). C-type inactivation can continue at a substantial rate as long as the activation gates are open, so the persistent binding of the inactivation particle effectively extends each depolarizing pulse by an extra time period during which C-type inactivation occurs.

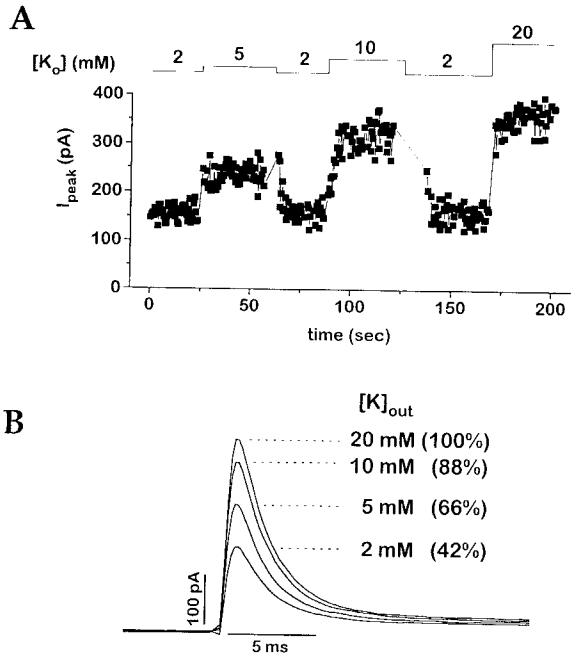

Figure 1. Peak Shaker K^+ Current at 2 Hz Is Very Sensitive to $[K^+]_{out}$

(A) The peak Shaker K^+ current in an outside-out patch is plotted for repeated pulses with several changes of $[K^+]_{out}$. Current was measured in response to a 20 ms depolarizing voltage step from −80 to +40 mV repeated every 0.5 s (2 Hz).

(B) Averaged current traces are shown for the indicated $[K^+]_{out}$. Traces were averaged during the steady-state period between the changes in $[K^+]_{out}$.

These two interactions between N- and C-type inactivation can quantitatively explain the variation in cumulative inactivation seen with changes in frequency and $[K^+]_{out}$. This variation of K^+ current inactivation with physiological changes in $[K^+]_{out}$ provides a mechanism by which neuronal electrical activity can be modulated by the changes in $[K^+]_{out}$ seen in neuronal tissue.

Results

Shaker K^+ Current during Repetitive Activity Is Very Sensitive to $[K^+]_{out}$

We examined the effect of $[K^+]_{out}$ on cumulative inactivation of wild-type Shaker K^+ channels (ShWT), using excised outside-out patches from transiently transfected HEK293 cells. To see the impact of cumulative inactivation on the peak K^+ current, we applied repeated depolarizing pulses at a rate of 2 per second. In each depolarizing voltage-clamp step from −80 to 0 mV, the Shaker channels activate rapidly and subsequently inactivate with a time constant of ~3 ms. Figure 1A plots the peak K^+ current for a series of pulses with varying $[K^+]_{out}$. The peak K^+ current is very sensitive to changes of $[K^+]_{out}$ between 2 and 20 mM. The steady-state peak current increases about 1.6-fold when $[K^+]_{out}$ is stepped from 2 to 5 mM, and 2.4-fold when $[K^+]_{out}$ is stepped from 2 to 20 mM (Figure 1B). This result is opposite to the expected change in the single-channel conductance, because raising $[K^+]_{out}$ should decrease, instead of increase, the driving force for K^+. Thus, the substantial increase in peak current with elevated $[K^+]_{out}$ is due to an increase in the number of activatable channels.

The effect of $[K^+]_{out}$ depends strongly on pulsing frequency. Figure 2A shows the peak current for three levels of $[K^+]_{out}$ (2, 5, and 10 mM), plotted for three different stimulation frequencies (0.125, 1, and 2 Hz). With low frequency stimulation (0.125 Hz), the peak current does not depend on $[K^+]_{out}$, but with increasing frequency, there is more reduction at low $[K^+]_{out}$. Conversely, an increase in stimulation frequency from 0.125 to 2 Hz reduces current by 74% in 2 mM $[K^+]_{out}$, but by only 36% in 10 mM $[K^+]_{out}$.

The Frequency-Dependent Effect of $[K^+]_{out}$ Depends on the Presence of Both C-Type and N-Type Inactivation

It seemed likely that the frequency- and $[K^+]_{out}$-dependent change in the number of available channels involved one of the two known inactivation mechanisms: N- or C-type inactivation. We tested channels with specific mutational defects in either N-type inactivation (ShΔ) or C-type inactivation (Sh-T449V; López-Barneo et al., 1993). Surprisingly, in both mutants the K^+-inhibited cumulative inactivation is abolished. ShΔ shows neither frequency dependence nor $[K^+]_{out}$ dependence (Figure 2B); Shaker T449V has no $[K^+]$ dependence and only a weak frequency-dependent reduction in current (Figure 2C). It thus appears that K^+-inhibited cumulative inactivation depends on the simultaneous presence of both C- and N-type inactivation. This behavior suggests that some kind of interaction between the two processes is responsible for the K^+-inhibited cumulative inactivation.

N-Type Inactivation Speeds C-Type Inactivation by Enhancing Its Sensitivity to Low $[K^+]_{out}$

Some interaction between N- and C-type inactivation has been seen by Hoshi et al. (1991); in the presence of N-type inactivation, C-type inactivation appears faster. Based on our observation that cumulative inactivation was very sensitive to $[K^+]_{out}$, we looked specifically at how this interaction varied with changes in $[K^+]_{out}$. We observed C-type inactivation in the presence of N-type inactivation by applying long depolarizing pulses. The Shaker K^+ current inactivates rapidly to ~2% of its peak value, the steady-state level for N-type inactivation; the remaining small current inactivates further with a relatively slow rate, as seen in Figures 3A and 3B. After the initial decline, N-type inactivation is in a rapid equilibrium compared with the slower inactivation process: this slower decline therefore represents the C-type inactivation rate of N-type inactivated channels (slightly contaminated by the inactivation rate of the 2% of channels open at steady-state). This C-type inactivation in the presence of N-type inactivation is dramatically different from C-type inactivation observed in isolation (cf. Figures 3B and 4A). At low $[K^+]_{out}$, C-type inactivation is greatly accelerated, whereas with high $[K^+]_{out}$ (160 mM), there is barely any C-type inactivation detectable. The rate of C-type inactivation titrates with the $[K^+]_{out}$ (Fig-

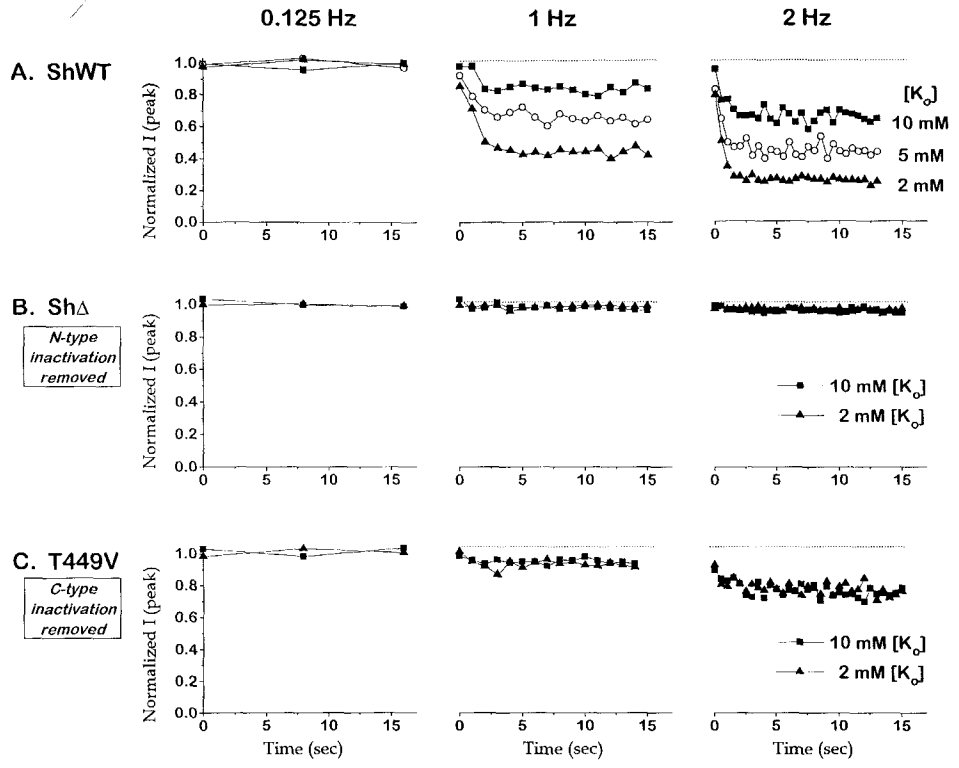

Figure 2. Frequency-Dependent Effect of $[K^+]_{out}$ in ShWT, ShΔ (N-Type Inactivation Removed), and Shaker T449V (C-Type Inactivation Removed)

The effects of changing the $[K^+]_{out}$ at different stimulating frequencies are shown for the Shaker H4 wild-type channel (ShWT; A), for ShΔ (Shaker Δ6–46, a mutation that removes N-type inactivation; B), and for Shaker T449V (a mutation that prevents C-type inactivation; C). Peak currents are plotted for 20 ms depolarizing pulses (-80 to 0 mV) repeated at different frequencies (0.125, 1, and 2 Hz) and with different $[K^+]_{out}$ (2–10 mM) in physiological saline in outside-out patches. The currents were normalized to the peak current obtained at 0.125 Hz. Similar results were obtained in at least two further experiments for each channel type.

ure 3C), showing a $K_{½}$ of 1.9 ± 0.3 mM with a maximal rate of 11.5 ± 0.6 s^{-1} at 0 $[K^+]_{out}$ and a minimal rate of 0.45 ± 0.04 s^{-1} at high $[K^+]_{out}$.

Eliminating Outward K^+ Flux Allows ShΔ to Inactivate Rapidly in Low $[K^+]_{out}$

How does C-type inactivation vary with $[K^+]_{out}$ when N-type inactivation is not present? Removing K^+_{out} has a relatively small effect on the rate of C-type inactivation in ShΔ (López-Barneo et al., 1993) (Figure 4A). One potential problem in detecting the K^+ sensitivity is generalized K^+ accumulation close to the membrane: indeed, very large currents tend to have even slower inactivation than small currents (data not shown). However, the absence of K^+ sensitivity is not due to overall K^+ accumulation, since ShΔ currents inactivate more slowly than ShWT currents in low $[K^+]_{out}$, even when the total ShΔ current is much smaller than the remnant ShWT currents, as seen in the ShΔ recording of Figure 4A with only about 15 active channels.

We do find, however, that the failure of ShΔ to inactivate rapidly in low $[K^+]_{out}$ is due to the efflux of K^+ through the channels. Under conditions that eliminate outward K^+ flux, the sensitivity to $[K^+]_{out}$ of ShΔ currents approaches that of ShWT. This can be seen in the two types of experiments in Figures 4B and 4C. In Figure 4B, we eliminate outward K^+ flux by removing all intracellular K^+ (K^+_{in}) and observing inward currents. The inward current with 5 mM $[K^+]_{out}$ inactivates much more quickly ($\tau \approx 400$ ms) than outward current with the same $[K^+]_{out}$ (or even 0 $[K^+]_{out}$; cf. Figure 4A). To measure the rate of inactivation with 0 $[K^+]_{out}$ and with no K^+ efflux, another strategy is needed. We temporarily remove the K^+_{in}, and then restore it to measure the fraction of channels that have inactivated (Figure 4C). At the beginning of the voltage step, no current is flowing because of the absence of K^+ on both sides of the membrane; then, after the solution is changed back to normal intracellular saline (with 160 mM $[K^+]$), the outward current appears almost instantaneously and then continues to inactivate. The envelope of these initial outward current peaks declines as the period of depolarization with 0 $[K^+]_{in}$ is prolonged, indicating the time course of inactivation (Figure 4C, symbols).

The rate of ShΔ C-type inactivation in the absence of any K^+ is about 4 s^{-1} at 0 mV, about one-third as fast as the rate of 11.5 s^{-1} measured for ShWT. The discrepancy is probably due to the shift in activation gating that occurs when K^+ is removed (Swenson and Armstrong, 1981; Shapiro and DeCoursey, 1991), since measurements made at +80 mV give a maximum rate in 0 $[K^+]_{out}$ of 11 ± 1 s^{-1} for ShΔ. By contrast, there is only minimal voltage dependence of ShWT inactivation (data not shown), so we suspect that the effect of the more depolarized voltage

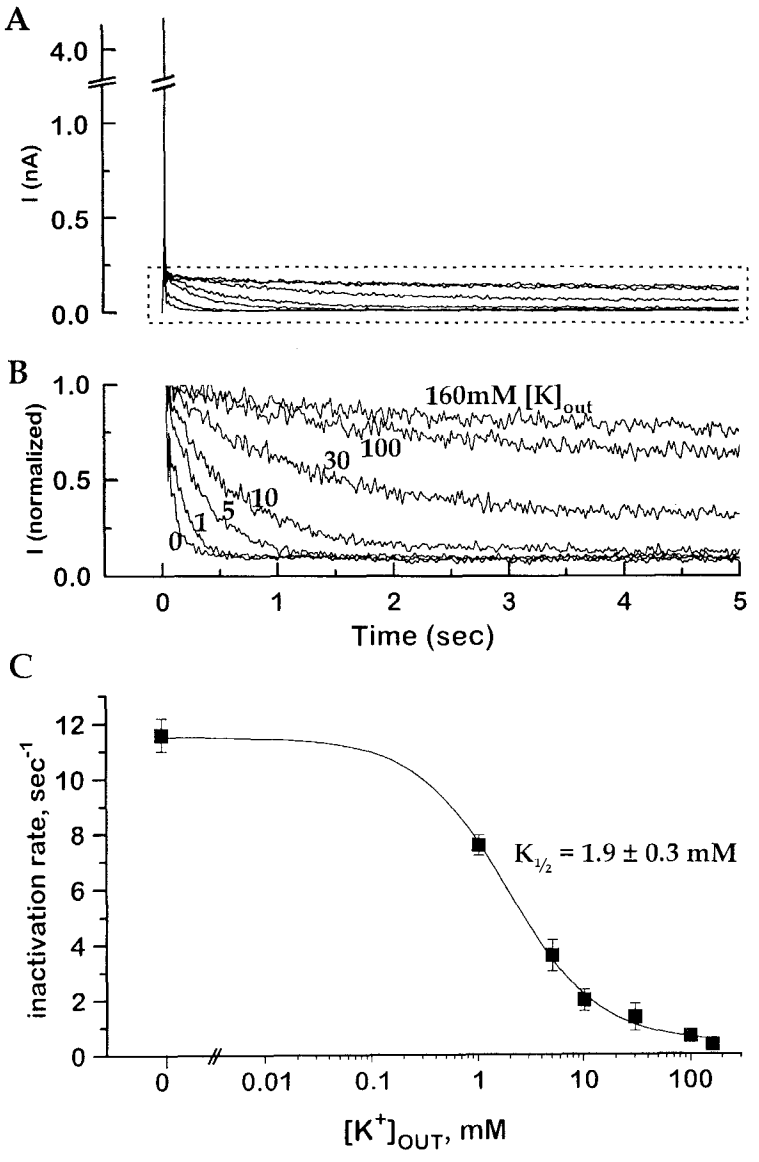

Figure 3. The Rate of C-Type Inactivation in the Presence of N-Type Inactivation Depends Steeply on $[K^+]_{out}$

(A) A typical experiment shows ShWT current during a 5 s depolarizing pulse (-80 to +40 mV) obtained in NMG-containing external solutions with different $[K^+]_{out}$. The current rapidly activates and inactivates (N-type inactivation), producing the large spike at the beginning of the pulse. Subsequently, the remaining ~2% of the channel inactivates relatively slowly (boxed part).

(B) The slowly inactivating fraction (boxed part in [A]) for each $[K^+]_{out}$ is shown, with all traces normalized to the same starting amplitude.

(C) C-type inactivation rate versus $[K^+]_{out}$ for ShWT, measured from single exponential fits to data collected as in (B). The points could be well fitted with the following logistic function: $[(R_{max} - R_{min})/(1 + [K^+]/K_{½})] + R_{min}$, with values R_{max} = 11.5 ± 0.6, R_{min} = 0.45 ± 0.04, and $K_{½}$ = 1.9 ± 0.3 mM. Each plotted rate represents the average and the SEM measured in at least three independent experiments. All rates reported are relaxation rates and are not corrected for the contribution of the recovery rate (this would make a difference only in the estimate of R_{min}). For display, traces in (A) and (B) were smoothed with an fast Fourier transform–based smoothing function with a 200 Hz cutoff frequency.

is to increase the open probability back to its normal value near one. Consistent with such a shift, we find that reducing $[K^+]_{out}$ produces a substantially faster deactivation rate at −80 mV.

A series of such measurements in the absence of K^+ efflux shows that, in ShΔ, C-type inactivation depends on K^+_{out} just as it does in ShWT. Using the inward current measurements in the range of 5–160 mM $[K^+]_{out}$ and the envelope measurement of Figure 4C at 0 and 1 mM (at +80 mV) gives a titration that agrees very well with the ShWT titration (Figure 4D). This indicates that C-type inactivation is governed by an ion binding site at or near the outer mouth of the channel, as previously suggested (Choi et al., 1991; Labarca and MacKinnon, 1992; López-Barneo et al., 1993). When this site is occupied by a K^+ ion or by TEA, C-type inactivation is extremely slow; when the site is empty, C-type inactivation is very fast. In the absence of N-type inactivation, the site is usually filled by the local accumulation of K^+ produced by flux through the channel. The presence of N-type inactivation blocks this flux and allows the C-type inactivation rate to be governed by the bulk $[K^+]_{out}$.

C-Type Inactivation Continues during Recovery from N-Type Inactivation

We suspected that the presence of N-type inactivation might affect C-type inactivation in yet another way. It is known that N-type inactivation slows the deactivation gating of Shaker channels. Under some circumstances, the rate-limiting step in channel deactivation after repolarization is the unbinding of the N-type ball (Demo and Yellen, 1991). If this holds true under the conditions of our experiments, then significant C-type inactivation (from the open,

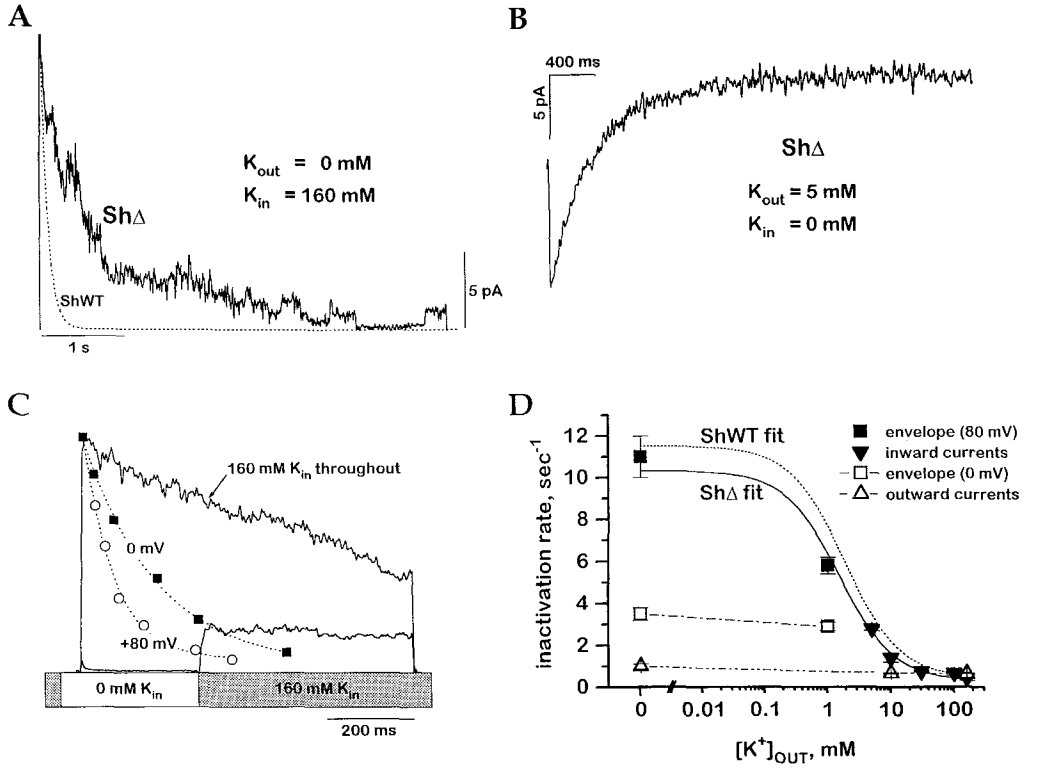

Figure 4. Eliminating Outward K^+ Flux Allows ShΔ to Inactivate Rapidly in Low $[K^+]_{out}$

(A) C-type inactivation of ShΔ currents in an outside-out patch containing about 15 channels, with an external solution containing 160 mM NMG and no added K^+ (V_m = +40 mV; $\tau \approx$ 740 ms). For reference, the dotted line shows the time course of ShWT inactivation with 0 $[K^+]_{out}$.

(B) Faster C-type inactivation in ShΔ for inward currents (i.e., with no K^+ efflux) measured with 5 mM $[K^+]_{out}$ and 0 K^+_{in} (V_m = 0 mV; $\tau \approx$ 400 ms).

(C) The "envelope" method for measuring C-type inactivation of ShΔ with 0 $[K^+]_{in}$ and, thus, no K^+ efflux. The $[K^+]_{in}$ was stepped from 0 mM (which prevents current flow) to 160 mM after depolarizing pulses of various durations. Two sample traces are shown from one experiment with 0 $[K^+]_{out}$. The upper trace was in the constant presence of 160 mM $[K^+]_{in}$. The lower trace was depolarized for 270 ms with 0 K^+_{in}, after which the 160 mM $[K^+]_{in}$ solution was restored. The square at 270 ms represents the peak current for this lower trace. A series of experiments at 0 mV (squares) and at +80 mV (circles) describe the time course of ShΔ inactivation in 0 K^+. The current traces were postfiltered with a fast Fourier transform-based smoothing function with a 200 Hz cutoff frequency.

(D) C-type inactivation rate versus $[K^+]_{out}$ for ShΔ with standard internal solution (open triangles) as in (A); ShΔ with 0 mM internal K^+, measured from decay of inward currents (closed inverted triangles), as in (B); and ShΔ with 0 mM $[K^+]_{in}$ (0 mV [open squares] and 80 mV [closed squares]) measured by the envelope method of (C). The solid line is the best fit to the closed symbols, with R_{max} = 10.3 ± 0.8, R_{min} = 0.3 ± 0.05, and $K_{½}$ = 1.5 ± 0.2 mM. The titration fit for the K^+ effect on ShWT is shown (dotted line) for reference. Each plotted rate represents the mean and SEM measured in at least three independent experiments (except for the 0 mV envelope data, which give the mean and range of two determinations).

N-type inactivated state) should occur not just during the brief depolarizing pulses but also for some additional time following the pulse, during the period of recovery from N-type inactivation.

We tested this prediction by measuring the amount of C-type inactivation induced by depolarizing pulses of different duration. Following the pulse, we allowed a recovery period of 300 ms at −80 mV (sufficient for most channels to recover from N-type inactivation) and then applied a second brief depolarizing pulse (Figure 5A, inset). The peak current in the second pulse, normalized to the peak current in the first, is approximately the fraction of channels that has not entered the C-type inactivated state. Figure 5A plots this measure of C-type inactivation as a function of the duration of the first pulse, for a series of experiments with 5 mM $[K^+]_{out}$.

As the pulse duration increases, C-type inactivation reduces the activatable fraction of channels exponentially, with a time constant of 330 ± 30 ms. This corresponds well to the time constant for C-type inactivation measured by the decline of the residual current during a long pulse (see Figure 3B). However, even for the briefest pulses, there is a substantial amount of C-type inactivation: for a 10 ms pulse, fully 44% of the channels enter the C-type inactivated state.

This remarkably large amount of C-type inactivation can be explained by the continuation of C-type inactivation after repolarization. We examined the fate of channels after a brief depolarizing pulse using a two-pulse recovery protocol (Figure 5B, top). Recovery occurs in two phases, fast and slow, corresponding to the lifetimes of the N- and C-type inactivated states, respectively. We describe the recovery time course using the following simple kinetic scheme:

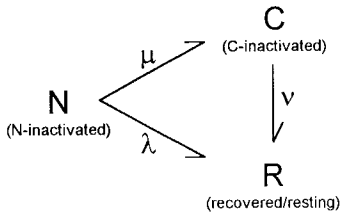

At the end of a brief pulse, essentially all of the channels are in the N-type inactivated state. These N-type inactivated channels have two possible fates (Figure 5C): they can recover directly to the R state (actually a collection of closed states) with rate λ, or they can enter the C-type inactivated state and then recover with the much slower rate ν. For simplicity, the model neglects the small amount of reinactivation from R to N and the possibility of recovery from C to N. As shown in Figure 5B (top), approximately half of the channels recover through each pathway, indicating that the two rates exiting the N-type inactivated state are roughly equal. In terms of the model, the time constant for the fast phase is $\tau_N = (\lambda + \mu)^{-1}$, and the fraction of channels recovering slowly is given by $f_c = \mu/(\lambda + \mu)$. This analysis gives values of $\lambda \approx 3.3\ s^{-1}$ and $\mu \approx 2.6\ s^{-1}$. Thus, after repolarization to −80 mV, the rate of C-type inactivation from the N-type inactivated state (μ) is approximately the same as it is during a long depolarizing pulse to 0 mV (3.3 s^{-1}; see Figure 3).

An alternative description of this effect is that, for a pulse of duration t, C-type inactivation occurs for a longer period ($t + T_{extra}$). Conceptually, this T_{extra} is the time period after the pulse for which C-type inactivation continues during recovery from N-type inactivation. The dotted exponential fit in Figure 5A gives a value of 240 ± 50 ms for T_{extra} (similar to the time constant for fast recovery). This means that a 10 ms pulse has an "inactivating power" of 250 ms. For the experiments of Figure 1 and under normal physiological circumstances, the membrane potential spends very little time at depolarized voltages; thus, the dominant route for C-type inactivation is from the N-type inactivated state that persists after a brief depolarization.

Discussion

How N-Type Inactivation Alters the K^+ Sensitivity of C-Type Inactivation

In the presence of N-type inactivation, we find that C-type inactivation is fast and very sensitive to $[K^+]_{out}$. In the absence of N-type inactivation, C-type inactivation in ShΔ is slow and rather insensitive to $[K^+]_{out}$. Our results suggest that there is a K^+_{out} site that controls C-type inactivation whether N-type inactivation is present or not, but that in the absence of N-type inactivation, this site is nearly always saturated (regardless of the bulk $[K^+]_{out}$) by K^+ flowing outward through the channel (Figure 6, $O^{(K)}$ state). N-type

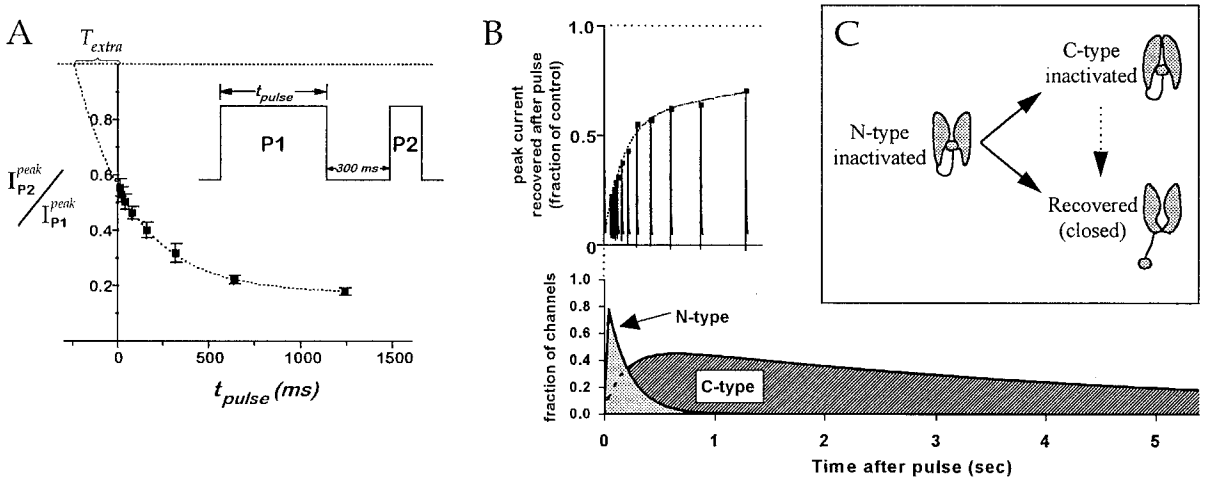

Figure 5. In ShWT, C-Type Inactivation Continues for an Additional Time after Repolarization

(A) To test whether C-type inactivation continues after repolarization, a two-pulse protocol (inset) was employed. A depolarizing pulse to 0 mV of variable duration (P1) was followed by a recovery period of 300 ms at -80 mV, to allow most N-type inactivation to recover; the extent of the inactivation remaining after this recovery period (mostly C-type) was tested with a second depolarizing pulse (P2). The ratio $I^{peak}_{P2}/I^{peak}_{P1}$ is plotted against the duration of P1. Every data point represents the mean and SEM of at least three different experiments with 5 mM $[K^+]_{out}$. The points are fitted to a monoexponential decay function giving a τ of 330 ± 30 ms and a y-intercept of 0.56. The effective extra time for C-type inactivation (T_{extra}) was estimated by back extrapolation of the exponential to a y value of 1 (corresponding to no inactivation); this gives a T_{extra} of 240 ± 50 ms. Data represent the mean and SEM of four experiments.

(B, top) Recovery from N-type inactivation was assessed by a two-pulse protocol in 5 mM $[K^+]_{out}$. Current was measured in response to a pair of depolarizing pulses (20 ms) from −80 to 0 mV separated by a hyperpolarizing recovery period (-80 mV) of varying duration (the time axis is shared with [B, bottom]). The peak current amplitudes were fitted to the sum of two exponentials. The time constants were 189 ± 3 ms for the fast component and 1700 ± 150 ms for the slow component; the fraction recovering by the fast component was 0.51 ± 0.07.

(B, bottom) Simulation of the time course of C-type inactivation during N-type recovery. The occupancy of the two inactivated states was modeled as described in the Experimental Procedures. Notice that C-type inactivation rises while N-type inactivation recovers, well after the end of the 5 ms pulse used in the simulation (invisible on this time scale). The C-type inactivated channels then recover over many seconds.

(C) Cartoon illustrating the alternative fates of N-type inactivated channels: recovery or C-type inactivation (see text).

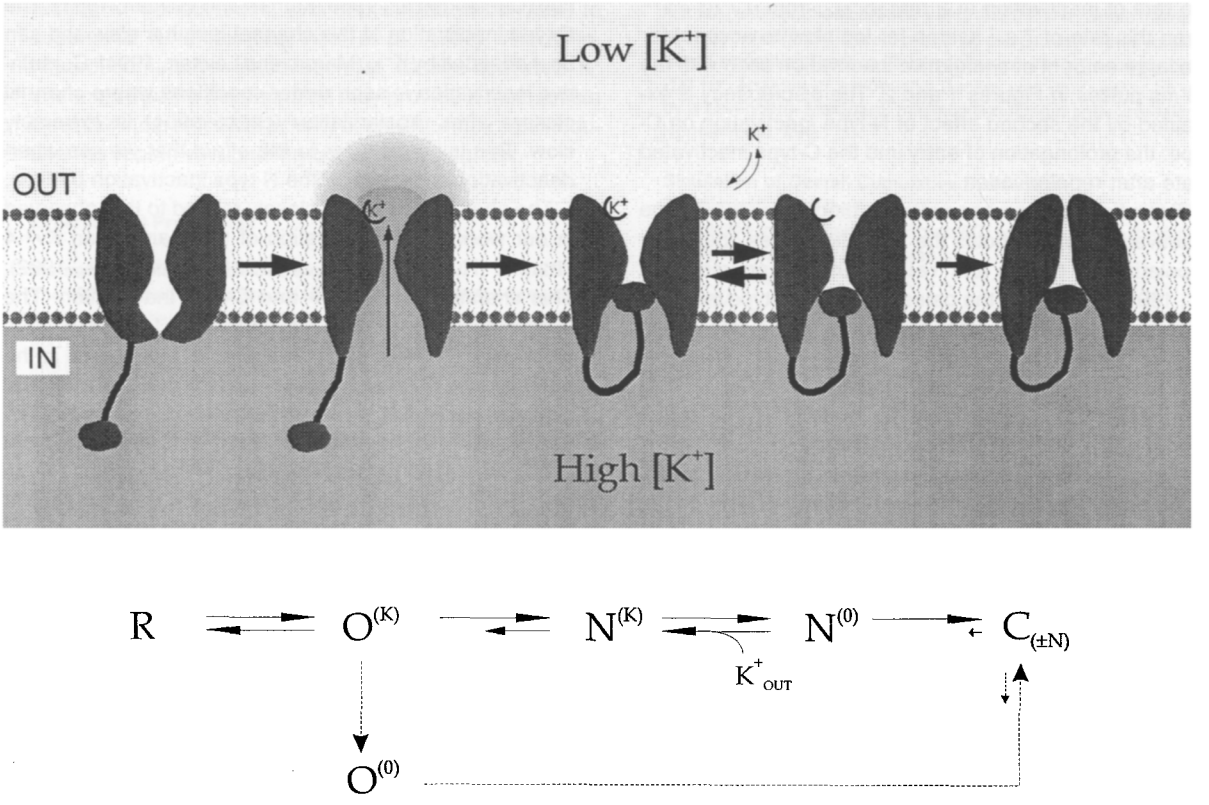

Figure 6. Model for the Mechanism of Coupling between N- and C-Type Inactivation: The Natural Course of Inactivation for a ShWT K^+ Channel.

Upon depolarization, the channel switches from the resting (R) to open (O) state. Efflux of K^+ through the open pore leads to a local increase in K^+_{out}, which keeps the external site controlling inactivation nearly saturated. The designation $O^{(K)}$ indicates the open state with K^+ bound to the external site. After opening, the N-type tethered inactivation ball can bind to the inner mouth of the channel and block current (the N-type inactivated [N] state). This N-type inactivated state has no K^+ efflux, so occupancy of the external site is controlled by the bulk $[K^+]_{out}$. C-type inactivation occurs rapidly only when the site is unoccupied, i.e., from the $N^{(0)}$ state. The kinetic scheme also indicates an alternate pathway to the C-type inactivated state, via the $O^{(0)}$ state. This state is entered only rarely, because of the high local $[K^+]$ under normal conditions of K^+ efflux, so the rate of C-type inactivation through this pathway is very slow. This slower pathway is the main pathway available for inactivation of ShΔ channels, which lack the N-type inactivation ball.

inactivation speeds up C-type inactivation and reveals its intrinsic K^+ sensitivity by preventing this outward K^+ flow and the consequent saturation of the site (Figure 6, $N^{(K)}$ and $N^{(0)}$ states).

This conclusion is supported by measurements in which the outward flow is eliminated not by N-type inactivation but instead by removing K^+_{in}. These experiments show that C-type inactivation in ShΔ, with no outward flux of K^+, is very fast with 0 $[K^+]_{out}$ and is inhibited by K^+_{out} in the same concentration range as the ShWT channel (see Figure 4). Interestingly, it appears that closure of the activation gate is affected by K^+_{out} in this same range (based on the voltage dependence in the low $[K^+]$ envelope experiments and other data on tail currents; data not shown), suggesting that the same site that controls C-type inactivation may also modulate channel closure (cf. Swenson and Armstrong, 1981; Marom and Levitan, 1994).

Although outward K^+ flux through the ShΔ channel can produce gross accumulation of $[K^+]_{out}$ in patches with particularly large currents, we think that the most important effect of outward flux occurs on a very local scale, in the extracellular mouth of an individual channel (illustrated in Figure 6 for the $O^{(K)}$ state). Even for the smallest macroscopic currents that we measure, in patches that contain only a dozen channels, the inactivation of ShΔ with 0 bulk K^+_{out} is very slow: the rates are consistent with an effective $[K^+]_{out}$ of ~15 mM. In single-channel experiments on C-type inactivation (e.g., Figure 1 in Hoshi et al., 1991), the inactivation rate is also very slow (<1 s^{-1}). This argues that K^+ efflux through an individual channel accumulates substantial K^+ at the external site controlling C-type inactivation. Only the elimination of K^+ efflux by removal of K^+_{in} or by the long-lasting blockade of the N-type inactivation particle can deplete the external mouth of K^+ enough to see a substantial sensitivity to bulk $[K^+]_{out}$. Our experiments in progress reveal that some intracellular blockers (but not others) mimic the effect of N-type inactivation on C-type. These studies with blockers should elucidate the mechanism of this K^+ deprivation effect further.

How the Interaction of N- and C-Type Inactivation Leads to Cumulative Inactivation

The increased $[K^+]_{out}$ sensitivity of C-type inactivation produced by N-type inactivation causes a large increase in

the rate of inactivation at 2 mM $[K^+]_{out}$, from 0.7 to 7 s^{-1}. Even this rate of 7 s^{-1} seems far too slow to account for the large amount of cumulative inactivation seen with the 20 ms pulses in Figures 1 and 2. The discrepancy is explained by the second effect of N-type inactivation on C-type: the prolongation of entry into the C-type inactivated state after repolarization.

This effect occurs because the binding of the N-type inactivation particle holds the activation gates open after repolarization (Demo and Yellen, 1991; Ruppersberg et al., 1991). As long as the gates are open, C-type inactivation can proceed at a rate very similar to the rate during the depolarizing pulse.

A simulation with a simple kinetic model helps to illustrate the situation (see Figure 5B, bottom). At the end of a brief pulse, very little C-type inactivation has occurred, and virtually all of the channels are in the N-type inactivated state. Upon repolarization, these channels do not close immediately, because of the binding of the inactivation particle. These N-type inactivated channels have two possible fates (see Figure 5C): the N-type particle may unbind and the channel close (N-recovery), or the N-type inactivated channel may proceed to the C-type inactivated state (C-inactivation). The partitioning into these two states depends on the relative rates of N-recovery and C-inactivation. Under the conditions of our experiment in Figure 5B, reproduced in the simulation, these two rates are about equal, so that half of the channels recover to the closed state and half end up in the C-type inactivated state. Notice that most of this C-inactivation occurs after the pulse (Figure 5B, bottom), during the extra effective inactivation time period described as T_{extra} in the experiment of Figure 5A.

The rates of both N-recovery and C-inactivation are sensitive to $[K^+]_{out}$, so that the partitioning of channels between the recovered and C-inactivated states is particularly K^+ sensitive. As $[K^+]_{out}$ is raised, the rate of C-type inactivation gets slower and the rate of N-type recovery gets faster (Demo and Yellen, 1991), reducing T_{extra}; both effects lead to less cumulative inactivation at high $[K^+]_{out}$. These two effects account quantitatively for the modulation of cumulative inactivation by frequency and $[K^+]_{out}$: the results of Figure 1 can be reproduced by simulation with the kinetic model (data not shown).

Relationship to Previous Work on Shaker and Other K^+ Channels

The effects of the interaction of N- and C-type inactivation have been seen before in studies on Shaker channels, in addition to the explicit study of the interaction by Hoshi et al. (1991). Studies of recovery from N-type inactivation at various $[K^+]_{out}$ showed an unexplained slow component at low $[K^+]$ (Hoshi et al., 1990; Demo and Yellen, 1991; Gómez-Lagunas and Armstrong, 1994). The result can be explained simply by supposing that, even for the brief pulses used in these studies, entry into the C-type inactivated state occurs at low $[K^+]_{out}$.

Cumulative inactivation has been studied in the mammalian Kv1.3 channel, which shows only C-type inactivation (Cahalan et al., 1985; Marom and Levitan, 1994). The C-type inactivation of this channel is rather slow and can be modulated by K^+_{out} (Marom and Levitan, 1994). Cumulative inactivation is seen under conditions where channel closure after repolarization (deactivation) is extremely slow. This is very similar to the effect that we see when deactivation is slowed by the N-type inactivation particle.

The phenomenon most closely related to that observed in our work is the inactivation of the mammalian Kv1.4 channel (Ruppersberg et al., 1991; Pardo et al., 1992). This channel has both N- and C-type inactivation. The C-type inactivation of Kv1.4 is particularly fast and K^+ sensitive; this is at least partly attributable to the lysine in the outer mouth (Shaker equivalent position 449), since the ShΔ mutant T449K shows very similar properties (López-Barneo et al., 1993). When N- and C-type inactivation coexist in Kv1.4, $[K^+]_{out}$ has two effects: at lower $[K^+]_{out}$, recovery from inactivation is much slower and the total current is less (Pardo et al., 1992). The effect on recovery is explained by the interaction we see in Shaker: at low K^+, more of the channels enter the slowly recovering C-type inactivated state. The reduction in peak current at low $[K^+]_{out}$ occurs also in the ShΔ mutant T449K (i.e., in the absence of N-type inactivation) and might be due to C-type inactivation of closed channels (López-Barneo et al., 1993).

Possible Physiological Implications

The mechanism of K^+-inhibited cumulative inactivation studied here in Shaker K^+ channels is sensitive to variation of $[K^+]_{out}$ in the physiological range and, thus, may have important consequences for electrical signaling. This significance is probably not limited to Drosophila muscle, where Shaker channels occur: several mammalian channels exhibit related phenomena. Most prominently, the mammalian Kv1.4 channel appears to show the same K^+ sensitivity, as previously highlighted by Pardo et al. (1992). The K^+-inhibited cumulative inactivation may not be limited, though, to K^+ channels like Kv1.4 that show dramatic, direct sensitivity of C-type inactivation to $[K^+]_{out}$. Even Kv1.3, whose intrinsic K^+ sensitivity is modest, may show a strong effect of K^+_{out}, if it becomes subject to N-type inactivation. This might occur by heteromultimerization with another channel subunit, or by assembly with the recently discovered β subunit of K^+ channels. The β subunits, which are generally not homologous to the pore-forming subunits, can confer N-type inactivation by assembly with a K^+ channel (Rettig et al., 1994).

In the cerebrospinal fluid bathing the brain, $[K^+]_{out}$ is generally tightly regulated at ~3 mM, but with high levels of neuronal excitation, it can rise as high as 6–10 mM (Sykova, 1983; Walz and Hertz, 1983). In the small extracellular space around individual neurons, elevated $[K^+]$ is probably even more common and possibly even larger (Frankenhaeuser and Hodgkin, 1956). Moreover, elevation of $[K^+]$ may occur not just through high levels of neuronal activity, but also through specific actions of neurotransmitters on glial cells. Glutamate released by neurons can depolarize glial cells; since glial cells have a large

resting K^+ conductance, this depolarization can lead to substantial K^+ efflux (MacVicar et al., 1988). The K^+-inhibited cumulative inactivation of voltage-activated K^+ channels that we have studied may provide a mechanism by which local electrical activity or glial K^+ efflux can modulate the repetitive signaling behavior of neurons.

Experimental Procedures

Mutants and Mammalian Cell Expression

The cDNA coding for the Shaker H4 (Kamb et al., 1988) wild-type and the mutants Shaker H4:Δ6–46 (Hoshi et al., 1990; Choi et al., 1991) and Shaker H4 T449V (MacKinnon and Yellen, 1990) were subcloned into the expression vector GW1-CMV (British Biotech, Cowley, Oxford, UK). For expression in mammalian cells, we used the human embryonic kidney 293 cell line (HEK293; American Type Culture Collection no. CRL-1533, Rockville, MD). Cultures were grown in Dulbecco's modified Eagle's medium (DMEM-F12; GIBCO BRL, Gaithersburg, MD) with 10% fetal bovine serum (Sigma Chemical, St. Louis, MO) to 40%–60% confluence and then split 1:3 one day before transfection. Cells for transfection were collected by treatment with 0.05% trypsin, 0.53 mM EDTA, washed once, and resuspended in HEPES-buffered saline at 2×10^6 cells/ml. Electroporation was done at 300–400 V (Electroporator, Invitrogen, San Diego, CA) in 0.4 cm cuvettes containing 200 μl of diluted cells, 25 μg of channel expression plasmid, 1 μg of an SV40 T antigen expression plasmid, and 3–5 μg of the CD8 expession plasmid, which encodes for the α subunit of the human CD8 lymphocyte surface antigen (generously provided by Dr. Brian Seed, Massachusetts General Hospital, Boston, MA). Cells were plated onto protamine-coated coverslips and maintained in growth medium at 37% with 5% CO_2 until use.

Visual Identification of Individual Transfected Cells

Transfected cells, which had been cotransfected with CD8 antigen were incubated with polystyrene microspheres that had been precoated with anti-CD8 antibody (Dynabeads M-450 CD8, Dynal, Great Neck, NY) for 10 min to 12 hr before use. Cells that express the CD8 antigen are decorated with many beads and are easily distinguishable from untransfected cells. Decoration and channel expression are well correlated (Jurman et al., 1994).

Excised Patch Recording

Excised outside-out and inside-out patch recordings were made using standard methods (Hamill et al., 1981), 20–72 hr after electroporation. Patch pipettes (1–3 MΩ) were coated with wax (Hygenic Corporation, Akron, OH). The standard internal solution contained 160 mM KCl, 1 mM EGTA, 0.5 mM $MgCl_2$, and 10 mM HEPES (pH 7.4); in the case of the experiments employing 0 K^+_{in}, K^+ was replaced with N-methylglucamine (NMG). The external solutions contained 150 mM NaCl, 3 mM $CaCl_2$, 1 mM $MgCl_2$, and 10 mM HEPES (pH 7.4; physiological saline), where KCl was added at the indicated concentration; and 160 mM NMG, 3 mM $CaCl_2$, 1 mM $MgCl_2$, and 10 mM HEPES (pH 7.4), where KCl was substituted for NMG as indicated. We have found no significant differences in inactivation between NMG- and Na^+-containing external solutions.

Most of the solution changes were done with a manual switch, which allows solution exchange in about 1 s. For fast solution exchange, we used the rapid perfusion method of solenoid-switched converging streams described by Brett et al. (1986), which achieved solution exchange in several milliseconds. The holding potential in all experiments was −80 mV; test potentials were as indicated. Saline-filled agarose (~0.6%) bridges connected the bath with an Ag-AgCl grounding wire.

Data Collection and Analysis

Control of membrane potential, perfusion, and data acquisition were performed on a 486-based PC, equipped with an AT-MIO-16F-5 analog interface (National Instruments, Austin, TX) using our own Windows-based software (VectorView; G. Y., unpublished). The currents were filtered at 3 kHz with an 8-pole Bessel filter (Frequency Devices, Haverhill, MA) and sampled between 1 kHz and 0.2 kHz. Some traces have been further digitally filtered for display using a fast Fourier transform–based smoothing function (Origin software) with a frequency cutoff of 200 Hz. Analysis of exponential decays was done either by eye or by a Levenberg–Marquardt minimization (Origin software, MicroCal, Northampton, MA).

Simulation of Overall Cumulative Inactivation

The simulations of the inactivation recovery (see Figure 6B) and the cumulative inactivation (see Figure 6C) were done with the following kinetic scheme and rate constants:

At 0 mV:

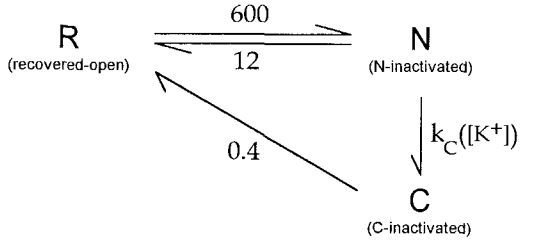

At −80 mV:

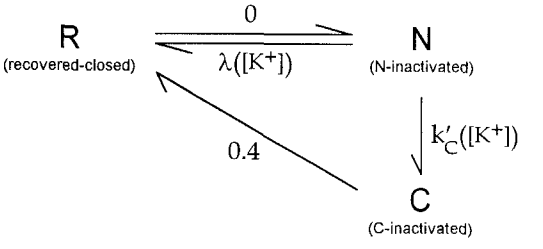

where $k_C([K^+])$ is the $[K^+]$-dependent rate of C-type inactivation, from Figure 3C; $k_C'([K^+])$ is that rate at −80 mV, set equal to $0.6 \times k_C([K^+])$; and $\lambda([K^+])$ is the $[K^+]$-dependent rate of N-type recovery, estimated to be $18\{[K^+]/([K^+] + 20\ mM)\}$. All rates are given in units of s^{-1}. The numerical simulation was done using MathCad 5.0+ (MathSoft, Cambridge, MA) to solve the eigenvector problem for the matrix solution to the Kolmogorov equations (Cox and Miller, 1972).

Acknowledgments

We are grateful to Mark Jurman for providing the transiently transfected cells, and to him, Yi Liu, and Miguel Holmgren for stimulating discussions. This project was supported by a National Institute of Neurological Disorders and Stroke grant (NS29693) to G. Y. and by a stipend from the Karl-Benz-Gottlieb-Daimler foundation to T. B.

The costs of publication of this article were defrayed in part by the payment of page charges. This article must therefore be hereby marked *"advertisement"* in accordance with 18 USC Section 1734 solely to indicate this fact.

Received May 3, 1995; revised June 22, 1995.

References

Aldrich, R.W., Getting, P.A., and Thompson, S.H. (1979). Mechanism of frequency-dependent broadening of molluscan neurone soma spikes. J. Physiol. *291*, 531–544.

Armstrong, C.M., and Bezanilla, F. (1977). Inactivation of the sodium channel. II. Gating current experiments. J. Gen. Physiol. *70*, 567–590.

Brett, R.S., Dilger, J.P., Adams, P.R., and Lancaster, B. (1986). A method for the rapid exchange of solutions bathing excised membrane patches. Biophys. J. *50*, 987–992.

Cahalan, M.D., Chandy, K.G., DeCoursey, T.E., and Gupta, S. (1985).

A voltage-gated potassium channel in human T lymphocytes. J. Physiol. *358*, 197–237.

Choi, K.L., Aldrich, R.W., and Yellen, G. (1991). Tetraethylammonium blockade distinguishes two inactivation mechanisms in voltage-activated K^+ channels. Proc. Natl. Acad. Sci. USA *88*, 5092–5095.

Connor, J.A., and Stevens, C.F. (1971). Prediction of repetitive firing behaviour from voltage clamp data on an isolated neurone soma. J. Physiol. *213*, 31–53.

Cox, D.R., and Miller, H.D. (1972). The Theory of Stochastic Processes (London: Chapman and Hall).

Demo, S.D., and Yellen, G. (1991). The inactivation gate of the *Shaker* K^+ channel behaves like an open-channel blocker. Neuron *7*, 743–753.

Frankenhaeuser, B., and Hodgkin, A.L. (1956). The after-effects of impulses in the giant nerve fibres of *Loligo*. J. Physiol. *131*, 341–376.

Gómez-Lagunas, F., and Armstrong, C.M. (1994). The relation between ion permeation and recovery from inactivation of *Shaker*B K^+ channels. Biophys. J. *67*, 1806–1815.

Grissmer, S., and Cahalan, M. (1989). TEA prevents inactivation while blocking open K^+ channels in human T lymphocytes. Biophys. J. *55*, 203–206.

Hamill, O.P., Marty, A., Neher, E., Sakmann, B., and Sigworth, F.J. (1981). Improved patch-clamp techniques for high-resolution current recording from cells and cell-free membrane patches. Pflügers Arch. *391*, 85–100.

Hille, B. (1992). Ionic Channels of Excitable Membranes. Second Edition (Sunderland, MA: Sinauer).

Hoshi, T., Zagotta, W.N., and Aldrich, R.W. (1990). Biophysical and molecular mechanisms of Shaker potassium channel inactivation. Science *250*, 533–538.

Hoshi, T., Zagotta, W.N., and Aldrich, R.W. (1991). Two types of inactivation in *Shaker* K^+ channels: effects of alterations in the carboxy-terminal region. Neuron *7*, 547–556.

Jurman, M.E., Boland, L.M., Liu, Y., and Yellen, G. (1994). Visual identification of individual transfected cells for electrophysiology using antibody-coated beads. BioTechniques *17*, 876–881.

Kamb, A., Tseng-Crank, J., and Tanouye, M.A. (1988). Multiple products of the Drosophila *Shaker* gene may contribute to potassium channel diversity. Neuron *1*, 421–430.

Labarca, P., and MacKinnon, R. (1992). Permeant ions influence the rate of C-type inactivation in Shaker K channels. Biophys. J. *61*, A378.

López-Barneo, J., Hoshi, T., Heinemann, S.H., and Aldrich, R.W. (1993). Effects of external cations and mutations in the pore region on C-type inactivation of Shaker potassium channels. Receptors and Channels *1*, 61–71.

MacKinnon, R., and Yellen, G. (1990). Mutations affecting TEA blockade and ion permeation in voltage-activated K^+ channels. Science *250*, 276–279.

MacVicar, B.A., Baker, K., and Crichton, S.A. (1988). Kainic acid evokes a potassium efflux from astrocytes. Neurosci. *25*, 721–725.

Marom, S., and Levitan, I.B. (1994). State-dependent inactivation of the Kv3 potassium channel. Biophys. J. *67*, 579–589.

Pardo, L.A., Heinemann, S.H., Terlau, H., Ludewig, U., Lorra, C., Pongs, O., and Stühmer, W. (1992). Extracellular K^+ specifically modulates a rat brain K^+ channel. Proc. Natl. Acad. Sci. USA *89*, 2466–2470.

Rettig, J., Heinemann, S.H., Wunder, F., Lorra, C., Parcej, D.N., Dolly, J.O., and Pongs, O. (1994). Inactivation properties of voltage-gated K^+ channels altered by presence of beta-subunit. Nature *369*, 289–294.

Ruppersberg, J.P., Frank, R., Pongs, O., and Stocker, M. (1991). Cloned neuronal I_K(A) channels reopen during recovery from inactivation. Nature *353*, 657–660.

Shapiro, M.S., and DeCoursey, T.E. (1991). Permeant ion effects on the gating kinetics of the type *L* potassium channel in mouse lymphocytes. J. Gen. Physiol. *97*, 1251–1278.

Swenson, R.P., and Armstrong, C.M. (1981). K^+ channels close more slowly in the presence of external K^+ and Rb^+. Nature *291*, 427–429.

Sykova, E. (1983). Extracellular K^+ accumulation in the central nervous system. Prog. Biophys. Mol. Biol. *42*, 135–189.

Walz, W., and Hertz, L. (1983). Functional interactions between neurons and astrocytes. II. Potassium homeostasis at the cellular level. Prog. Neurobiol. *20*, 133–183.

Yellen, G., Sodickson, D., Chen, T.-Y., and Jurman, M.E. (1994). An engineered cysteine in the external mouth of a K^+ channel allows inactivation to be modulated by metal binding. Biophys. J. *66*, 1068–1075.

Zagotta, W.N., Hoshi, T., and Aldrich, R.W. (1990). Restoration of inactivation in mutants of Shaker K^+ channels by a peptide derived from ShB. Science *250*, 568–571.